



Isoflavone derivatives inhibit NF- κ B-dependent transcriptional activity

Sunhee Lee^a, Kyung Chan Lim^b, Soon Young Shin^c, Young Han Lee^{c,*}

^a Division of Bioscience and Biotechnology, Konkuk University, Seoul 143-701, Republic of Korea

^b Shrine High School, Royal Oak, MI 48073, USA

^c Institute of Biomedical Science and Technology, RCTC, Konkuk University, Seoul 143-701, Republic of Korea

ARTICLE INFO

Article history:

Received 3 August 2010

Revised 17 August 2010

Accepted 18 August 2010

Available online 22 August 2010

Keywords:

Isoflavone

NF- κ B

TNF α

QSAR

ABSTRACT

The transcription factor NF- κ B regulates diverse biological activities, such as inflammatory responses, cell proliferation, and cell survival. Isoflavones are known to have anti-inflammatory and anti-tumor activities, due, in part, to inhibition of NF- κ B activity. However, the structural moiety of isoflavones responsible for the inhibition of NF- κ B is not clearly understood. In this work, structure–activity relationships of isoflavone derivatives were examined with regard to NF- κ B inhibition, using CoMFA and CoMSIA. The results show that substituents at the C-7 and C-4' positions are crucial for the inhibition of TNF α -induced transcriptional activity of NF- κ B.

© 2010 Elsevier Ltd. All rights reserved.

NF- κ B is a pivotal transcription factor that regulates the expression of a variety of proteins that promote inflammatory responses, including pro-inflammatory cytokines, chemokines, cyclooxygenase 2, matrix metalloproteinases,¹ and carcinogenesis.² NF- κ B exists as either a homodimer or heterodimer, and is composed of several subunits, including NF- κ B1 (p50/p105), NF- κ B2 (p52/p100), RelA (p65), RelB, and c-Rel.³ NF- κ B activation is tightly controlled through the proteolysis of I κ B proteins, a family of endogenous inhibitors.⁴ In resting cells, NF- κ B is present in the cytoplasm in an inactive form, bound to I κ B proteins.⁵ In response to various stimuli, I κ B kinase (IKK) is activated and phosphorylates I κ B. The phosphorylated I κ B is then ubiquitinated and degraded through a proteasome-dependent pathway,⁶ resulting in the release of NF- κ B. The released NF- κ B immediately translocates to the nucleus where it activates target genes promoters, encoding cytokines, growth factors, cell adhesion molecules, and anti-apoptotic proteins.^{7,8} Although appropriate NF- κ B activation is important for normal cellular proliferation and immune responses, deregulated activation of NF- κ B has been linked to diverse inflammatory disorders, such as autoimmune arthritis, septic shock, lung fibrosis, asthma, and atherosclerosis.⁹ In addition to a role in the inflammatory responses, aberrant activation of the NF- κ B pathway has been identified in tumor microenvironments and has been implicated in the development of some human cancers.^{2,10,11} Indeed, high levels of NF- κ B are frequently observed in association with, among others, breast, ovarian, uterine cervix, prostate, skin, esophagus, and colon cancers.¹² There is accumulating evidence that compounds

that suppress the NF- κ B pathway, such as glucocorticoids and aspirin, can reduce inflammatory responses and act as therapeutic agents in the treatment of inflammation and cancer.¹² Some isoflavones, such as genistein and puerarin (8-C-glucoside of daidzein), have been shown to inhibit NF- κ B activation.^{13–15} However, the relationship between the structure of a given isoflavone and the inhibition of NF- κ B activity is not well understood. The goal of this investigation was to analyze the structure–activity relationships (SAR) of isoflavone derivatives and to identify the structural moiety responsible for their anti-inflammatory effects.

One of the well-known pathways that activate NF- κ B is the tumor necrosis factor α (TNF α) receptor-mediated signaling pathway.¹⁶ TNF α is a pro-inflammatory cytokine, that is, produced by a variety of cell types, including immune cells, endothelial cells, fibroblasts, and neuronal tissues.¹⁷ TNF α regulates cell proliferation, differentiation, apoptosis, and immune responses, and also plays a critical role in tumor invasion and metastasis.^{18–20} This Letter details the effects of 23 isoflavone derivatives on the inhibition of TNF α -induced NF- κ B activation and correlates isoflavone activity with three-dimensional quantitative structure–activity relationships (3D-QSAR).

Isoflavone derivatives were purchased from Indofine Chemical Co. Inc. (Hillsborough, NJ). Inhibitory potency was evaluated by measuring the NF- κ B-dependent transcriptional activity using the NF- κ B *cis*-acting luciferase reporter system. Briefly, HCT116 cells were transiently transfected with 5 \times NF- κ B-Luc reporter plasmid for 72 h, followed by the addition of 10 ng/mL TNF α in the absence or presence of each tested compound (10 μ M). After 12 h, the cells were collected and the NF- κ B-dependent transcriptional activity was measured using a luciferase activity assay.²¹

* Corresponding author. Tel.: +82 2 2049 6115; fax: +82 2 3437 9781.

E-mail address: yhlee58@konkuk.ac.kr (Y.H. Lee).

Isoflavones have a C6–C3–C6 skeleton (A-, C-, and B-rings), where C6–C3 comprise a 4*H*-chromen-4-one and C6 corresponds to a benzene ring attached at the C3 position. The structures of these isoflavone derivatives and their inhibitory effects on NF- κ B-dependent transcription induced by TNF α are listed in Table 1.

Although all of the isoflavones contain the same core structure, the observed biological activities against TNF α -induced NF- κ B activation varied, most likely due to the varying substituents. To identify the SAR responsible for the inhibition of NF- κ B, 3D-QSAR was performed using the Sybyl 7.3 software. Twenty-three compounds were divided into two groups: a training set used to generate QSAR models, and a test set (compounds **1** and **20** in Table 1) used to validate the models.

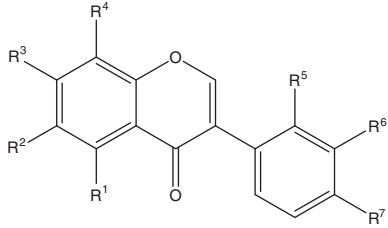
The structures in Table 1 were constructed based on the X-ray crystallographic structure of 4'-hydroxy-7-methoxyisoflavone used as a ligand for chalcone *O*-methyltransferase (PDB code 1FP2).²³ The first two rings of the C6–C3–C6 skeleton constitute a 4*H*-chromen-4-one. Thus, 3D structures of all the compounds could be built using the molecular mechanics algorithms provided by Sybyl 7.3. Each structure was subjected to energy minimization, terminated upon the convergence of total energy (0.05 kcal/mol Å). Because there is a rotational bond between the C-ring and B-ring, systematic conformational searches were performed in Sybyl to determine the conformer with the lowest energy.

All compounds were aligned using the Sybyl/DATABASE Alignment module. In the alignment procedure, 5,7,3',4'-tetramethoxyisoflavone, which exhibited the highest inhibitory activity, was used as a template and the atom-based root mean square (rms) fit method was adapted with the Sybyl/DATABASE ALIGN option.²² Aligned structures are given in the Supplementary data.²⁴

A training set was used for comparative molecular field analyzes (CoMFA).²² The model showing the best cross-validated correlation coefficient ($q^2 = 0.789$) was chosen for further analyzes. Partial least square (PLS) analyzes were performed to establish a linear relationship between the biological activity and the resulting field matrix of the compounds. The cross-validated analyzes were performed using the leave-one-out (LOO) method. The final non-cross-validated ($r^2 = 0.913$) analysis was performed using the optimal number of components (2) obtained from the LOO method. In the PLS analysis, the standard error of estimate and *F* values were 0.196, and 94.879, respectively. The best CoMFA model was obtained using a region-focusing method. CoMFA models were evaluated by predicting the activities of each compound, based on the model, and comparing the predictions with experimental data.²⁴ Residuals between the experimental and predicted values for the training set ranged from 0.009 (1.7%) to 0.422 (40%).²⁴ Because the biological data used in this experiment were obtained from cell-based assays, the error range may be larger than that obtained with a molecular assay. To validate the QSAR model, two derivatives were selected as a test set.

To visualize the relationship between structure and activity, CoMFA contour maps were generated using Sybyl 7.3. The steric and electrostatic field descriptors contributed 25.6% and 74.4%, respectively. Of the steric field contributors, the bulky favored and disfavored regions contributed 22% and 78%, respectively (Fig. 1). The bulky favored region consisted of the 5-position of the A-ring, the 3'-positions of the B-ring, and the 2-position of C-ring; the bulky disfavored region included the 7-position of the A-ring. Of the electrostatic field contributors, the electronegative and electropositive favored regions contributed 17% and 83%,

Table 1
Structure of 23 isoflavone derivatives and biological activity



	Nomenclature	R ¹	R ²	R ³	R ⁴	R ⁵	R ⁶	R ⁷	Biological activity
<i>Training set</i>									
2	5,4'-Dihydroxy-7-methoxyisoflavone	OH	H	OMe	H	H	H	OH	0.34
3	3',4'-Dimethoxy-7-hydroxyisoflavone	H	H	OH	H	H	OMe	OMe	2.53
4	6,4'-Dimethoxy-7-hydroxyisoflavone	H	OMe	OH	H	H	H	OMe	2.37
5	5,7,3',4'-Tetramethoxyisoflavone	OMe	H	OMe	H	H	OMe	OMe	0.19
6	6,7,3',4'-Tetramethoxyisoflavone	H	OMe	OMe	H	H	OMe	OMe	0.40
7	7,8,4'-Trihydroxyisoflavone	H	H	OH	OH	H	H	OH	1.22
8	7,8,4'-Trimethoxyisoflavone	H	H	OMe	OMe	H	H	OMe	0.95
9	7,3',4'-Trimethoxyisoflavone	OH	H	H	H	H	H	H	0.45
10	4'-Bromo-5,7-dimethoxyisoflavone	OMe	H	OMe	H	H	H	Br	0.25
11	6-Chloro-7-methylisoflavone	H	Cl	Me	H	H	H	H	0.32
12	2'-Chloro-5,7-dimethoxyisoflavone	OMe	H	OMe	H	Cl	H	H	0.54
13	3'-Chloro-5,7-dimethoxyisoflavone	OMe	H	OMe	H	H	Cl	H	0.63
14	4'-Chloro-5,7-dimethoxyisoflavone	OMe	H	OMe	H	H	H	Cl	0.61
15	6-Chloro-4',7-dimethoxyisoflavone	H	Cl	OMe	H	H	OH	OMe	0.54
16	4'-Chloro-7-hydroxy-8-methylisoflavone	H	H	OH	Me	H	H	Cl	1.04
17	4'-Chloro-7-methoxy-8-methylisoflavone	H	H	OMe	Me	H	H	Cl	0.63
18	2',6-Dichloro-7-methoxyisoflavone	H	Cl	OMe	H	Cl	H	H	0.54
19	4',7-Dimethoxy-8-methylisoflavone	H	H	OMe	Me	H	H	OMe	0.62
21	7-Methoxy-8-methylisoflavone	H	H	OMe	Me	H	H	H	0.23
22	7-Methyl-2',4',6-trichloroisoflavone	H	Cl	Me	H	Cl	H	Cl	0.27
23	5-Methyl-7-methoxyisoflavone	Me	H	OMe	H	H	H	H	0.67
<i>Test set</i>									
1	7-Methoxyisoflavone	H	H	OMe	H	H	H	H	0.36
20	7-Hydroxy-8-methylisoflavone	H	H	OH	Me	H	H	H	0.45

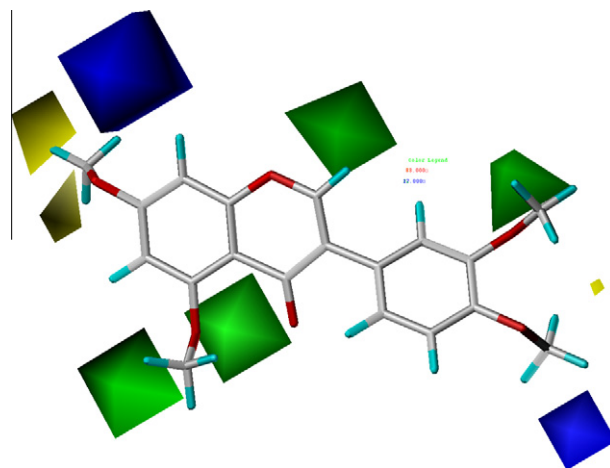


Figure 1. CoMFA contour maps. The corresponding steric and electrostatic field contributions were 25.6% and 74.4%, respectively. The steric field contours are shown in green (more bulk-favored) and yellow (less bulk-favored), while the electrostatic field contours are shown in red (electronegative substituent-favored) and blue (electropositive substituent-favored).

respectively. The electropositive region contained the 7-position of the A-ring and the 4'-position of the B-ring.

Comparative molecular similarity indices analyzes (CoMSIA) were used to calculate contour maps (Fig. 2), describing the steric and electrostatic fields as well as the hydrophobic, and hydrogen bond (H-bond) donor and acceptor fields.²² A partial least squares (PLS) analysis was used to determine correlations between biological activity and descriptors of the physicochemical properties of each compound. The model displaying the best cross-validated value ($q^2 = 0.540$) was selected for further analyzes. The corresponding r^2 was 0.970. The number of components, the standard error of estimate, and F value were 6, 0.130, and 76.652, respectively. The CoMSIA calculations revealed steric, electrostatic, and H-bond acceptor fields contributions of 14.9%, 61.8%, and 23.2%, respectively. Of the steric contributions, the steric bulky favored region contributed 5% and the disfavored region, 95%. The bulky disfavored region contained the 8-position of the A-ring. In the electrostatic field, the electronegative-favored region contributed 79% and

the electropositive-favored region, 21%.²⁵ The electropositive region contained the 7-position of the A-ring. The steric and electrostatic contour maps from these CoMSIA analyzes were generally in accordance with the CoMFA contour maps. Thus, the CoMSIA results focused on the H-bond acceptor field. The hydrophobic field consisted of H-bond acceptor-favored and -disfavored regions, contributing 95% and 5%, respectively. The H-bond acceptor-favored region contained the 7-position of the A-ring; the H-bond acceptor-disfavored region was near the 4'-positions of the B-ring.

The inhibitory activity of isoflavones was further demonstrated with 5,7,3',4'-tetramethoxyisoflavone, which was most effective in inhibiting TNF α -induced NF- κ B activity. Its effect on TNF α -induced nuclear translocation of NF- κ B was examined by Western blot analysis.²⁶ The level of p65 NF- κ B in the nuclear fraction induced by TNF α was significantly reduced by pretreatment with 5,7,3',4'-tetramethoxyisoflavone (Fig. 3A). Furthermore, 5,7,3',4'-tetramethoxyisoflavone also prevented TNF α -induced mRNA expression of NF- κ B target genes, such as CXC motif ligand 1 (CXCL1), X-linked inhibitor of apoptosis (XIAP), and mammalian IAP homolog C (CIAP2; Fig. 3B–D), as revealed by reverse transcription-polymerase chain reaction (RT-PCR) analyzes.²⁷ These results suggest that isoflavones prevent NF- κ B-dependent transcriptional activity induced by TNF α .

Based on the results obtained from CoMFA and CoMSIA analyzes, a possible binding site for isoflavones is shown in Figure 4. Although there is no information about the target of isoflavone activity, it can be inferred that R³ of the A-ring and R⁷ of B-ring require electrostatic sites, while the oxygen atom of the C-ring, R³ of A-ring, and R⁷ of B-ring represent H-bonding sites.

In conclusion, a QSAR study of isoflavone derivatives revealed that the substituents at C-7 and C-4' are necessary for controlling NF- κ B-dependent transcriptional activation induced by TNF α . NF- κ B is an attractive molecular target in controlling diverse disorders because various inflammatory stimuli can activate NF- κ B and aberrant activation is involved in a variety of pathogenesises, including inflammatory disorders and tumor development.²⁸ Indeed, isoflavone derivatives, such as genistein and daidzein, are known to protect against breast cancer, prostate cancer, and osteoporosis.^{29–31} Thus, isoflavone derivatives that inhibit the TNF α -induced transcriptional activation of NF- κ B may represent promising

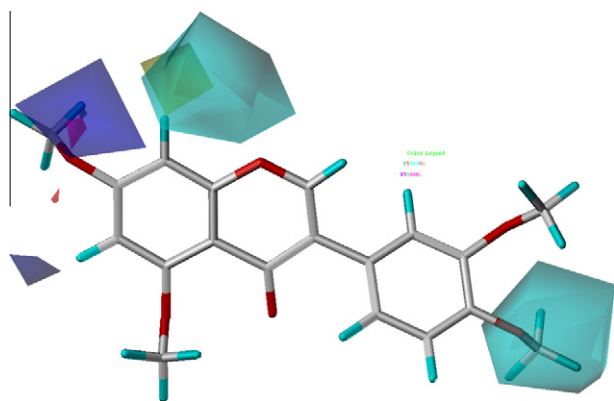


Figure 2. CoMSIA contour maps show contributions from more bulk-favored (green), less bulk-favored (yellow), electronegative-favored (red), electropositive-favored (blue), H-bond acceptor-favored (magenta), and H-bond acceptor (cyan) regions. The corresponding field contributions of steric, electrostatic, and H-bond acceptor fields were 14.9%, 61.8%, and 23.2%, respectively.

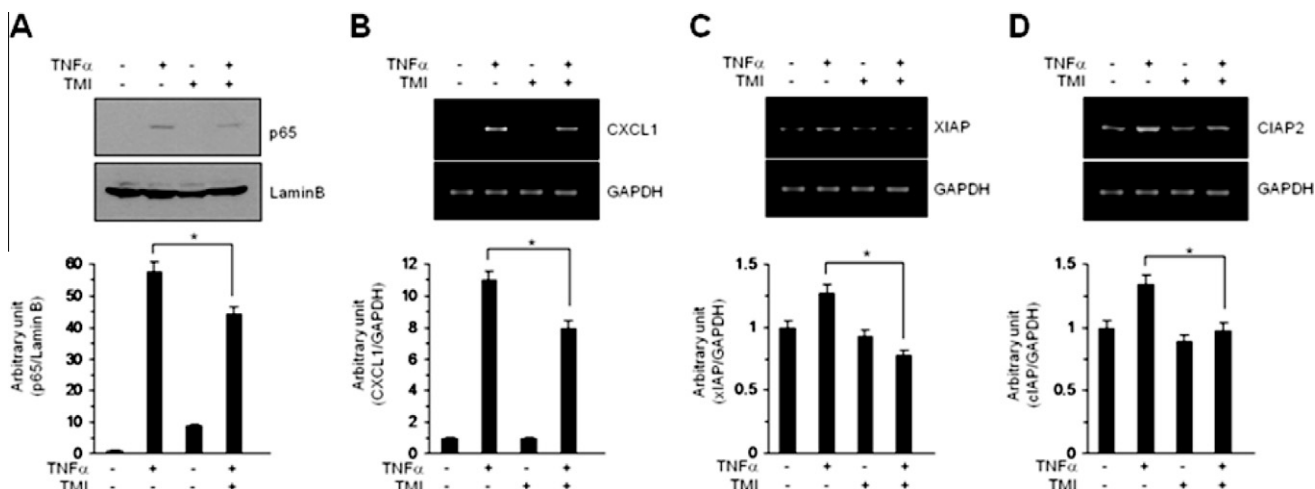


Figure 3. The effect of 5,7,3',4'-tetramethoxyisoflavone (TMI) on the inhibition of TNF α -induced NF- κ B activity is shown. (A) Effect of 5,7,3',4'-tetramethoxyisoflavone on the level of p65 NF- κ B in the nuclear fraction. The effects of 5,7,3',4'-tetramethoxyisoflavone on the mRNA expression of NF- κ B target genes (B) CXCL1, (C) XIAP, and (D) CIAP2. The results are presented as the mean, with error bars representing one standard deviation ($n = 6$, $P < 0.05$).

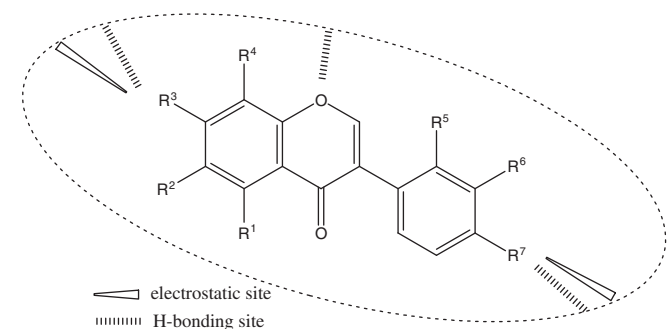


Figure 4. A molecular binding diagram deduced from CoMFA and CoMSIA results. and denote electrostatic and H-bonding sites, respectively.

chemopreventative or chemotherapeutic agents. The current QSAR study of isoflavones may be useful in the development of new compounds for controlling inflammatory disorders and cancer.

Acknowledgments

This work was supported by a Disease Network Research Program Grant (NRF, 20090084183). S.L. and K.C.L. contributed equally to this work.

Supplementary data

Supplementary data associated with this article can be found, in the online version, at doi:10.1016/j.bmcl.2010.08.089.

References and notes

- Barnes, P. J.; Karin, M. *N. Engl. J. Med.* **1997**, *336*, 1066.
- Karin, M.; Cao, Y.; Greten, F. R.; Li, Z. W. *Nat. Rev. Cancer* **2002**, *2*, 301.
- Ghosh, S.; May, M. J.; Kopp, E. B. *Annu. Rev. Immunol.* **1998**, *16*, 225.
- Sun, S. C.; Ley, S. C. *Trends Immunol.* **2008**, *29*, 469.
- Tang, E. D.; Inohara, N.; Wang, C. Y.; Nuñez, G.; Guan, K. L. *J. Biol. Chem.* **2003**, *278*, 38566.
- Miyamoto, S.; Seufzer, B. J.; Shumway, S. D. *Mol. Cell. Biol.* **1998**, *18*, 19.
- Subramaniam, D.; Giridharan, P.; Murmu, N.; Shankaranarayanan, N. P.; May, R.; Houchen, C. W.; Ramanujam, R. P.; Balakrishnan, A.; Vishwakarma, R. A.; Anant, S. *Cancer Res.* **2008**, *68*, 8573.
- Karin, M.; Lin, A. *Nat. Immunol.* **2002**, *3*, 221.

- Baldwin, A. S. *Annu. Rev. Immunol.* **1996**, *14*, 649.
- Pikarsky, E.; Porat, R. M.; Stein, I.; Abramovitch, R.; Amit, S.; Kasem, S.; Gutkovich-Pyest, E.; Urieli-Shoval, S.; Galun, E.; Ben-Neriah, Y. *Nature* **2004**, *431*, 461.
- Karin, M. *Nature* **2006**, *441*, 431.
- Yamamoto, Y.; Gaynor, R. B. *J. Clin. Invest.* **2001**, *107*, 135.
- Davis, J. N.; Kucuk, O.; Sarkar, F. H. *Nutr. Cancer* **1999**, *35*, 167.
- Valachovicova, T.; Slivova, V.; Bergman, H.; Shuherk, J.; Sliva, D. *Int. J. Oncol.* **2004**, *25*, 1389.
- Li, Y.; Sarkar, F. H. *Clin. Cancer Res.* **2002**, *8*, 2369.
- Gaur, U.; Aggarwal, B. B. *Biochem. Pharmacol.* **2003**, *66*, 1403.
- Xu, T.; Lundqvist, A.; Ahmed, H. J.; Eriksson, K.; Yang, Y.; Lagergård, T. *Microbes Infect.* **2004**, *6*, 1171.
- Coussens, L. M.; Werb, Z. *Nature* **2002**, *420*, 860.
- Joyce, J. A.; Pollard, J. W. *Nat. Rev. Cancer* **2009**, *9*, 239.
- Balkwill, F. *Nat. Rev. Cancer* **2009**, *9*, 361.
- HCT116 human colon cancer cells (American Type Culture Collection) were maintained in DMEM medium supplemented with 10% fetal bovine serum (Hyclone). NF- κ B-dependent transcription was measured with a *cis*-acting reporter assay system. HCT116 cells were seeded onto 12-well plates and transfected with 0.5 μ g of pNF- κ B-Luc, which contains five repeats of NF- κ B binding sites (Stratagene), using LipofectamineTM 2000 (Invitrogen) according to the manufacturer's protocol. To monitor transfection efficiency, 50 ng of the pRL-null plasmid encoding renilla luciferase (Promega) was included in all samples. At 72 h post-transfection, levels of firefly and renilla luciferase activity were measured sequentially from a single sample of cells, either untreated or treated with 10 ng/mL TNF α in the absence or presence of the test compound for 12 h, using the Dual-GloTM Luciferase Assay System (Promega). The normalized level of luciferase activity in the TNF α -only treated sample was designated as 1.22.
- Lee, S.; Woo, Y.; Shin, S. Y.; Lee, Y. H.; Lim, Y. *Bioorg. Med. Chem. Lett.* **2009**, *19*, 2116.
- Zubieta, C.; He, X. Z.; Dixon, R. A.; Noel, J. P. *Nat. Struct. Biol.* **2001**, *8*, 271.
- Data not shown in the text can be found in the Supplementary data.
- The field contributions for the analysis of CoMFA and CoMSIA contour maps were determined based on matching the physicochemical properties of the template showing the best biological activity with the field descriptors used.
- HCT116 cells were treated with 5,7,3',4'-tetramethoxyisoflavone for 30 min, followed by the addition of TNF α for 30 min. Cells were harvested and the nuclear fractions were collected. Total nuclear lysates (20 μ g) were separated by 10% SDS-PAGE and transferred to nitrocellulose filters. The filters were blocked with 5% non-fat dry milk and were probed with primary antibodies, anti-p65 NF- κ B antibody (Santa Cruz Biotechnology), and anti-lamin B antibody (Santa Cruz Biotechnology). Lamin B was used as a marker for the nuclear fraction. Positive reactions were visualized with an enhanced chemiluminescence plus Western blotting detection system (Amersham Bioscience).
- HCT116 cells were treated with 5,7,3',4'-tetramethoxyisoflavone for 30 min, followed by addition of TNF α for 18 h. Total RNA was extracted using a Trizol RNA extraction kit (Invitrogen). The first-strand cDNA was synthesized from 500 ng of total RNA using an iScript cDNA synthesis kit (Bio-Rad). For RT-PCR analyses, gene-specific primers for CXCL1 (forward, 5'-atggccgcgcgtctctctcc-3'; reverse, 5'-gtggattgtcactgttcag-3'), XIAP (forward, 5'-acaccatatacccgaggaaac-3'; reverse, 5'-cttgcatctgtcttctgagc-3'), CIAP2 (forward, 5'-cctgtgtgtaaatctgccttg-3'; reverse, 5'-caattcgccaccataactctg-3'), and GAPDH (forward, 5'-tcgacagtca

- gccgcatttc-3'; reverse, 5'-cgcccaatagaccacctccg-3') were used. The PCR conditions for all primers were as follows: hold for 5 min at 94 °C, followed by 30 cycles of denaturation at 94 °C (30 s), annealing at 55 °C (30 s), and elongation at 72 °C (1 min). The amplified products were separated by electrophoresis on a 1% agarose gel.
28. Lee, C. H.; Jeon, Y. T.; Kim, S. H.; Song, Y. S. *BioFactors* **2007**, 29, 19.
29. Zhang, Y.; Chen, W. F.; Lai, W. P.; Wong, M. S. *Inflammopharmacology* **2008**, 16, 213.
30. Helferich, W. G.; Andrade, J. E.; Hoagland, M. S. *Inflammopharmacology* **2008**, 16, 219.
31. Molinié, B.; Georgel, P. *Drug News Perspect.* **2009**, 22, 247.